Inorganic Chemistry

ARTICLE

pubs.acs.org/IC

Switching of Molecular Insertion in a Cyclic Molecule via Photo- and Thermal Isomerization

Satoshi Umeki, Shoko Kume, and Hiroshi Nishihara*

Department of Chemistry, School of Science, The University of Tokyo, 7-3-1, Hongo, Bunkyo-ku 113-0033, Japan

Supporting Information

ABSTRACT:

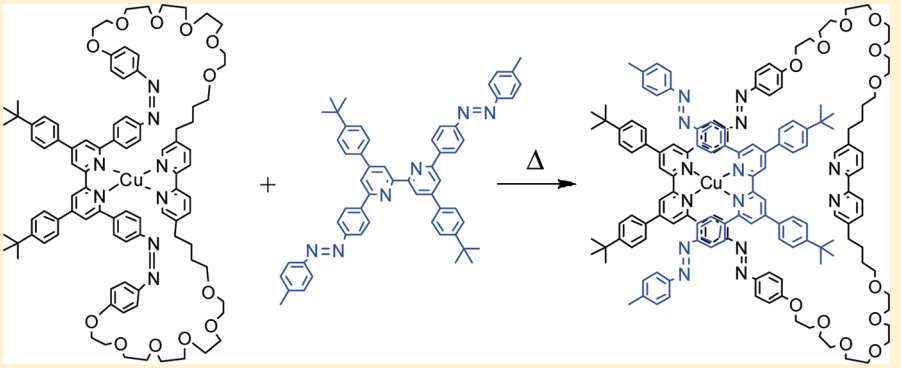

Two new cyclic ligands were synthesized: a ligand with two *trans*-azobenzene moieties and one bipyridine moiety, *trans*$_2$-*o*AB-O13, and a ligand with two *trans*-azobenzene moieties and two bipyridine moieties, *trans*$_2$-*o*AB-bpy. Both ligands underwent reversible trans-cis isomerization at the azobenzene moieties. The mole ratios of the *trans*$_2$ form:*trans-cis* form:*cis*$_2$ form, evaluated by ^{1}H NMR spectroscopy of the photostationary states prepared by 1 h illumination, were 0.13:0.27:0.60 (365 nm irradiation) and 0.41:0.47:0.12 (436 nm irradiation) for *o*AB-O13, and 0.18:0.12:0.70 (365 nm irradiation) and 0.36:0.43:0.21 (436 nm irradiation) for *o*AB-bpy. When *trans*$_2$-*o*AB-O13 was mixed with Cu(I), both the bipyridine units and the polyether chains coordinated to the copper center. Addition of a noncyclic bipyridine ligand, *trans*$_2$-*o*AB-2OH, afforded a bis(bipyridine)copper(I) complex, [Cu(*trans*$_2$-*o*AB-O13)(*trans*$_2$-*o*AB-2OH)]BF_4. The bis(bipyridine) ligand, *trans*$_2$-*o*AB-bpy, formed a 1:1 complex with Cu(I), [Cu(*trans*$_2$-*o*AB-bpy)]BF_4. [Cu(*cis*$_2$-*o*AB-bpy)]BF_4 did not undergo the ligand substitution reaction with a noncyclic ligand with two azobenzene moieties and one bipyridine moiety, *o*AB, whereas its thermal isomerization in the presence of *o*AB caused the formation of [Cu(*trans*$_2$-*o*AB-bpy)(*trans*$_2$-*o*AB)]BF_4, indicating that the isomerization and ligand exchange reactions synchronized via a conformational change of the cyclic ligand.

INTRODUCTION

Molecular machines have attracted much attention in nanoscale research, and their development has been accompanied by the introduction of new technologies for handling and assembling functional molecules.[1] The construction of molecular machines via combination and synchronization of molecular modules with well-characterized responses constitutes an efficient design strategy.[2] One of the examples of the molecular modules is azobenzene. The large conformational change through the reversible photoisomerization of azobenzenes can be used as a mechanical motion of molecular machines.[3] We have studied photochromic metal complexes, in which photochromic organic ligands are coordinated to transition metals. These complexes show unique physical and chemical properties.[4] We developed a photoelectric conversion system based on the ligand exchange reaction between a copper complex containing azobenzene-appended bipyridine ligands (*o*ABs) and free bipyridines (bpys). Ligand exchange was modulated by the reversible photoisomerization of the azobenzene moieties (Figure 1).[5]

We also achieved acid−base-responsive photoisomerization of a copper complex containing OH^- groups attached to azobenzene-appended bipyridine ligands, *o*AB-2OH.[6] In the present study, we synthesized new cyclic ligands based on the *o*AB structure, one ligand with a polyether chain, *o*AB-O13, and the other ligand with a polyether chain linked by an additional bpy moiety, *o*AB-bpy (Figure 2). In these cyclic structures, the ability to coordinate Cu(I) was controlled by changing the cycle's structure by photoisomerization of the azobenzene moieties. In this study, we examined the relationship between isomerization and coordination of *o*AB-O13 and *o*AB-bpy to Cu(I) and found that isomerization of the *o*AB-bpy complex created a binary structure in which one moiety was either inserted or removed from the coordination sphere formed by the cycle (Scheme 1). We describe the synthesis and characterization of the cyclic

Received: January 21, 2011
Published: May 05, 2011

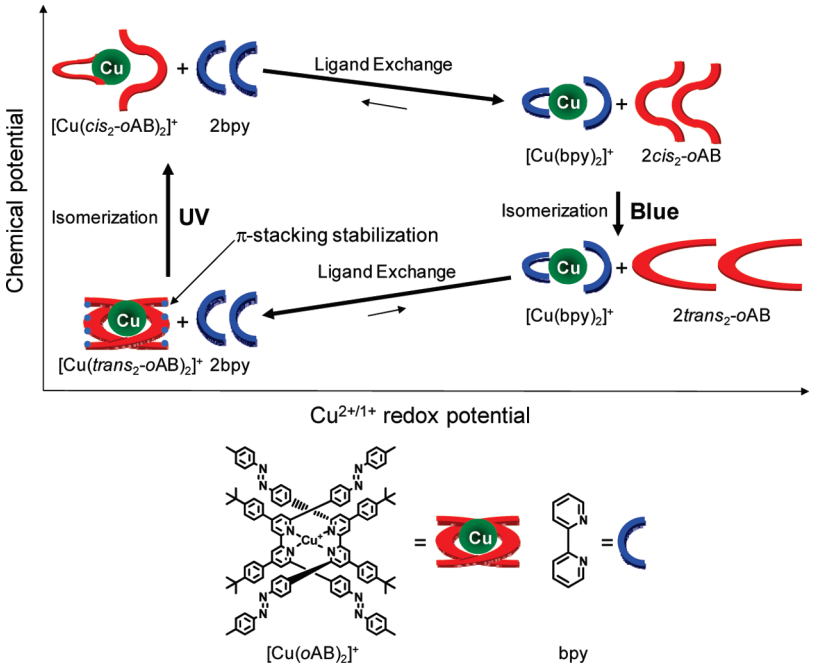

Figure 1. Photoelectric conversion system composed of $[Cu(oAB)_2]BF_4$.

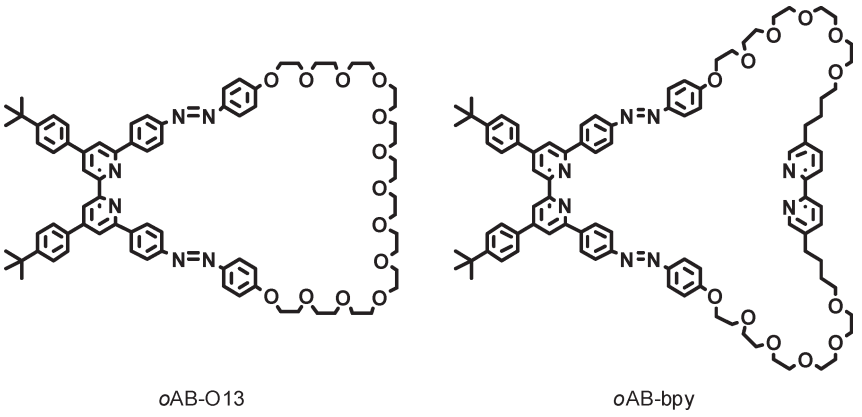

Figure 2. *o*AB-O13 and *o*AB-bpy.

ligands, their isomerization behavior, and their coordination to a Cu(I) center.

RESULTS AND DISCUSSION

Synthesis. The synthesis of the cyclic compound, *o*AB-O13, was carried out under dilute conditions (see Scheme 2 and the Experimental Section) to prevent polymerization. The reaction produced *o*AB-O13 by the reaction of *o*AB-2OH and O13-Ts in a ratio of 1:1, in addition to various byproducts from the reaction of *o*AB-2OH and O13-Ts in a ratio of 2:2, 3:3, and so forth. The products could be separated by gel permeation chromatography (GPC). *o*AB-bpy was synthesized by the same procedure (see Scheme 3 and the Experimental Section).

Comparison between the ^{1}H NMR spectra of *o*AB-2OH and *o*AB-O13 in $CDCl_3$ (see Supporting Information, Table S1) indicated that the peak corresponding to H*i* was shifted downfield after cyclization from 6.97 ppm to 7.09 ppm, upon transformation from an alcohol to an ether. The peak corresponding to H*d* was shifted dramatically upfield from 8.90 ppm to 8.21 ppm, suggesting that the bipyridine moieties underwent a conformational change via cyclization. Normal bipyridine derivatives, including *o*AB-2OH, are in the trans conformation because of steric hindrance at H*d*. However, steric hindrance between the ^{t}Bu groups and the polyether chains was even stronger in the trans conformation of the bipyridine moiety of *o*AB-O13 (Figure 3), making the cis conformation thermodynamically more favorable. The conformations of isomers in Figure 3 were estimated with minimized steric energy using the MM2 force-field method. The arrow in Figure 3 represents that the polyether chain cannot rotate around the *o*AB moiety because of the steric hindrance between the ^{t}Bu group and the polyether chain. This conformational change of the bipyridine moiety shifted the H*d* signal upfield because of steric repulsion. A similar upfield shift was observed in *o*AB-bpy, in which the bipyridine moieties were even more strongly constrained to the cis conformation (Supporting Information, Table S2).

dx.doi.org/10.1021/ic200145h |*Inorg. Chem.* 2011, 50, 4925–4933

Scheme 1. Schematic Presentation of the Coordination of *o*AB-O13 (a) and *o*AB-bpy (b) to Cu(I)

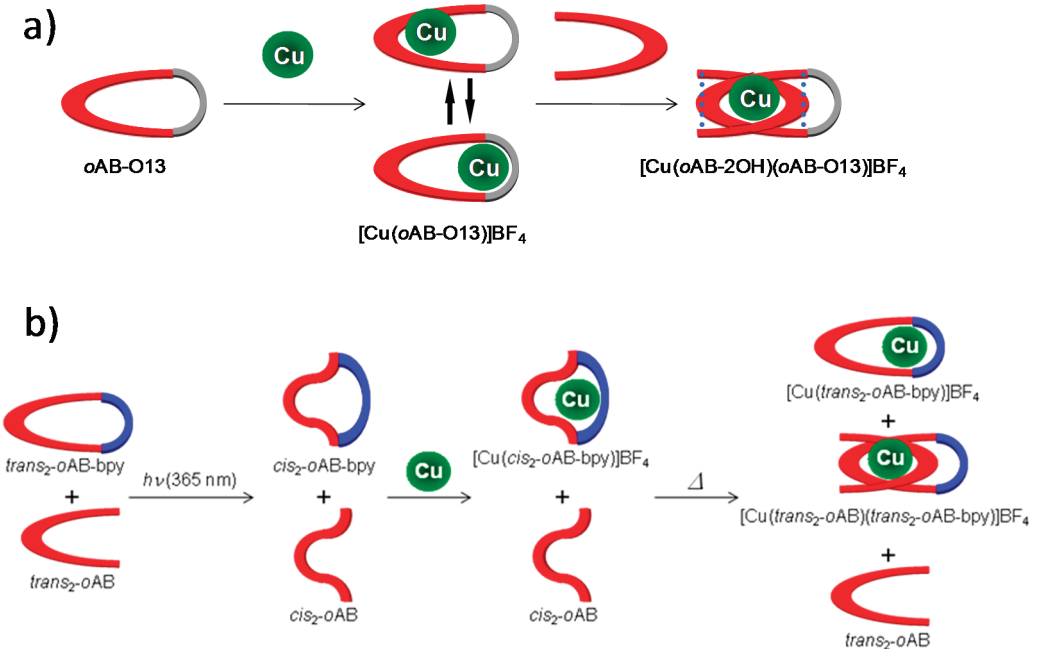

Scheme 2. Synthesis of *o*AB-O13

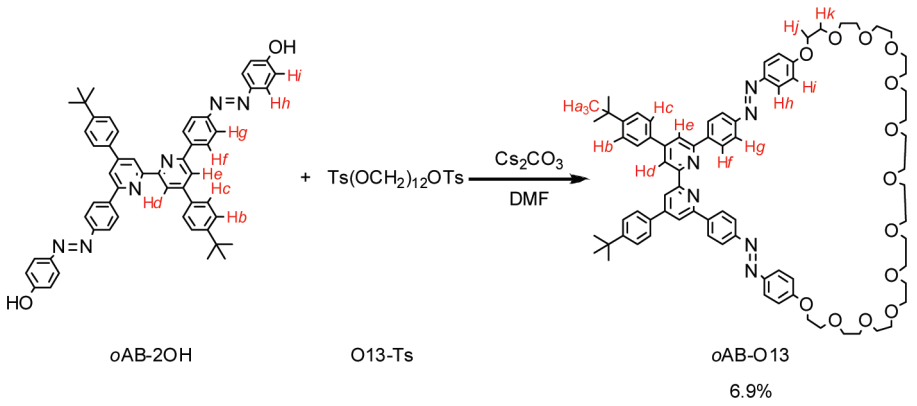

Isomerization of *o*AB-O13. The photoisomerization behavior of *o*AB-O13 in CD_2Cl_2 was monitored by ^1H NMR measurements (Figure 4). Before irradiation, *o*AB-O13 was present in the *trans*$_2$ form. New signals were observed upon 365 nm light irradiation, indicating a trans-to-cis isomerization. Both the *cis*$_2$ form and the *cis-trans* form were observed, and isomerization occurred through the *cis-trans* form. The ratios of the *trans*$_2$ form, the *cis-trans* form, and *cis*$_2$ form were 0.13:0.27:0.60. Isomerization in the reverse direction was achieved upon 436 nm irradiation. The solution reached a reversible dynamic photostationary state upon irradiation with 365 or 436 nm light for 1 h. The ratios of the *trans*$_2$ form, the *cis-trans* form, and the *cis*$_2$ form after irradiation with 436 nm light were 0.41:0.47:0.12. The original state (100% *trans*$_2$ form) was recovered upon heating the solution at 40 °C in the dark for 12 h.

Comparison between the ^1H NMR spectra of *trans*$_2$-*o*AB-O13 and *cis*$_2$-*o*AB-O13 in CD_2Cl_2 (see Supporting Information, Table S3) indicated that the signal of H*d* was shifted downfield from 8.54 ppm to 8.87 ppm because of the trans-to-cis isomerization, which altered the conformation of the bipyridine moiety. The bipyridine moiety of *trans*$_2$-*o*AB-O13 was in the cis conformation, as noted above. In contrast, because the tension in the ring was relieved through the trans-to-cis isomerization of the azobenzene moieties, the bipyridine moiety of *cis*$_2$-*o*AB-O13 was in the trans conformation, which had less steric hindrance. This conformational adjustment shifted the H*d* signal downfield. The bipyridine moiety of *cis-trans*-*o*AB-O13 was also in the trans conformation, and its H*d* signal was near to that of *cis*$_2$-*o*AB-O13 (see Figure 3). On the other hand, trans-to-cis isomerization shifted all signals upfield, except for the signal of H*d*. The upfield shift resulted from the shielding effects of the proximal aromatic rings, brought together by the trans-to-cis isomerization. The fact that the H*g* (from 8.11 ppm to 7.04 ppm) and H*h* (from 7.99 ppm to 6.99 ppm) shifts, which were nearest the azo moiety, showed large upfield shifts of more than 1 ppm, supports this conclusion.

dx.doi.org/10.1021/ic200145h |*Inorg. Chem.* 2011, 50, 4925–4933

Scheme 3. Synthesis of *o*AB-bpy

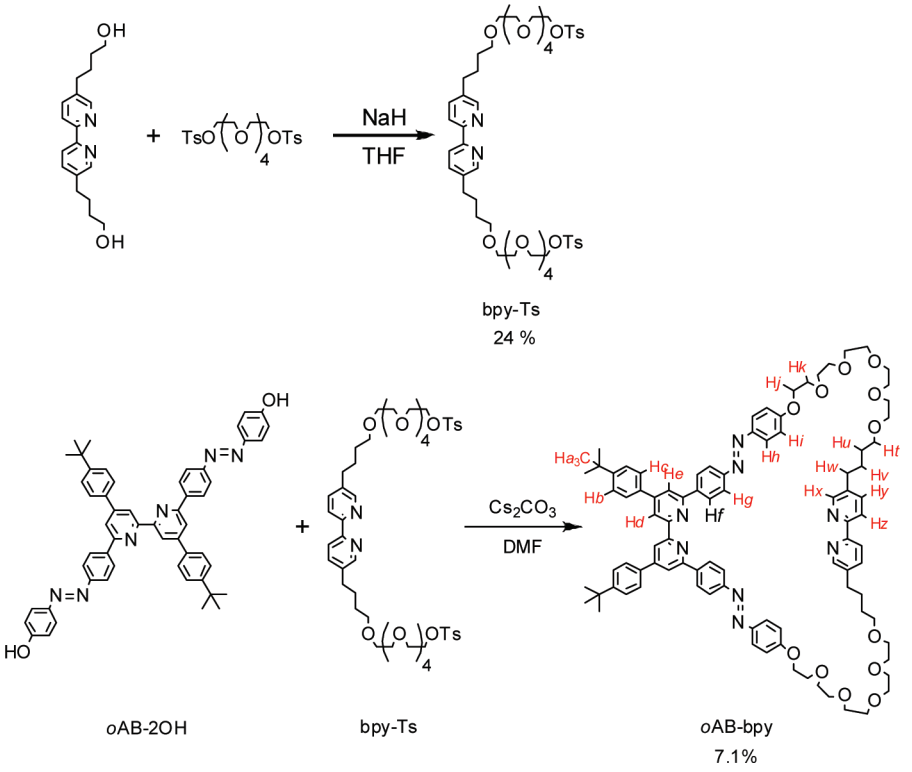

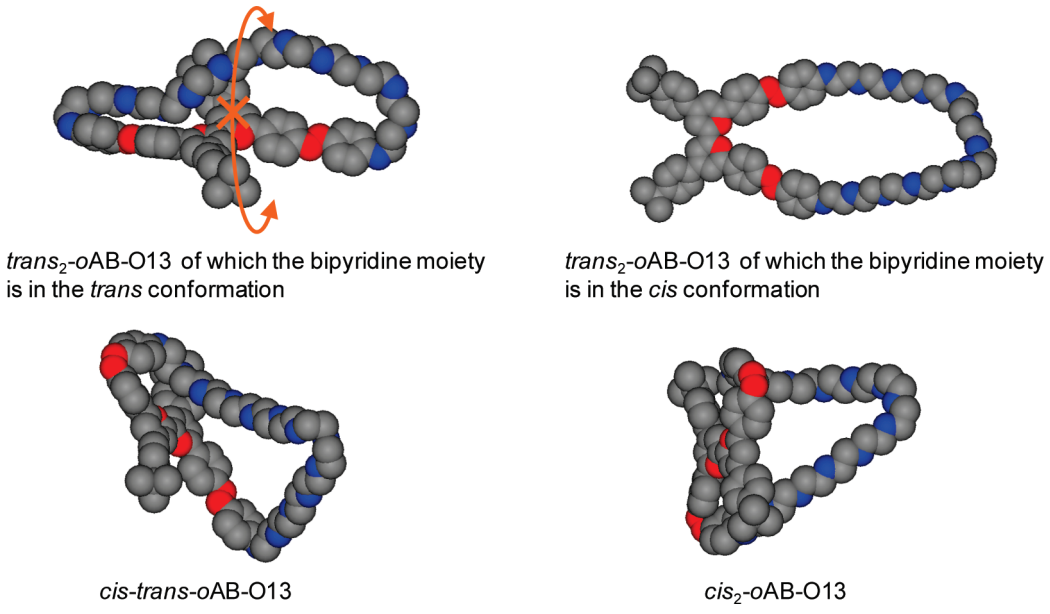

Figure 3. Molecular models of the isomers of *o*AB-O13 estimated with minimized steric energy using the MM2 force-field method (ChemBio3D 11.0).

The thermal cis-to-trans isomerization at 25 °C in the dark was monitored by ^{1}H NMR analysis, from which the ratio of each isomer was obtained (Supporting Information, Figure S1). Isomerization from the cis form to the trans form proceeded with the passage of time. The rate constant associated with isomerization from *cis*$_2$-*o*AB-O13 to *cis-trans-o*AB-O13, k_1, and the rate constant associated with isomerization from *cis-trans-o*AB-O13 to *trans*$_2$-*o*AB-O13, k_2, were estimated to be 8.0×10^{-5} s^{-1} and 1.3×10^{-5} s^{-1}, respectively (see the Supporting Information). k_1 was found to be larger than k_2. That is, isomerization from *cis*$_2$-*o*AB-O13 to *cis-trans-o*AB-O13 was faster than isomerization from *cis-trans-o*AB-O13 to *trans*$_2$-*o*AB-O13. Most likely, the *trans*$_2$-*o*AB-O13 conformation was thermally unstable to the extent that the bipyridine moiety was in the cis conformation and steric repulsion was significant (vide supra).

dx.doi.org/10.1021/ic200145h |*Inorg. Chem.* 2011, 50, 4925–4933

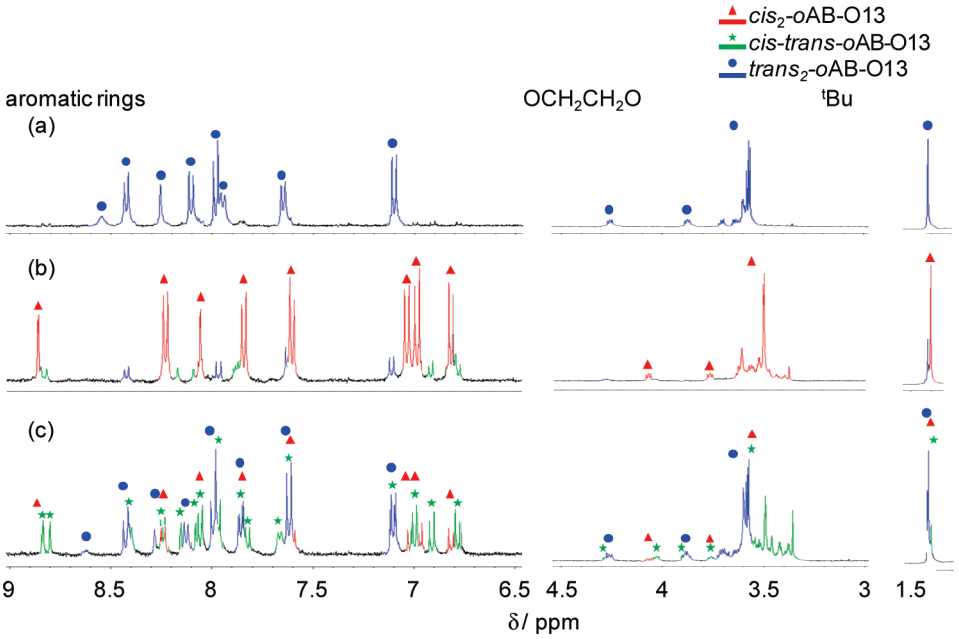

Figure 4. ^{1}H NMR spectral changes of *o*AB-O13 (1.5×10^{-3} M) in CD_2Cl_2 (a) initially, (b) after irradiation at 365 nm for 1 h, and (c) after further irradiation at 436 nm for 1 h.

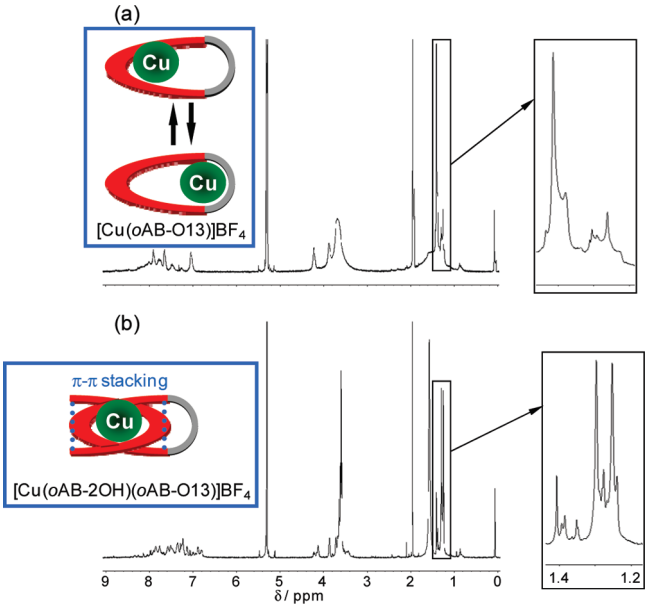

Figure 5. ^{1}H NMR spectral changes of *o*AB-O13 (1.0×10^{-3} M) and $[Cu(CH_3CN)_4]BF_4$ (1.0×10^{-3} M) in CD_2Cl_2 (a) initially and (b) after addition of *o*AB-2OH.

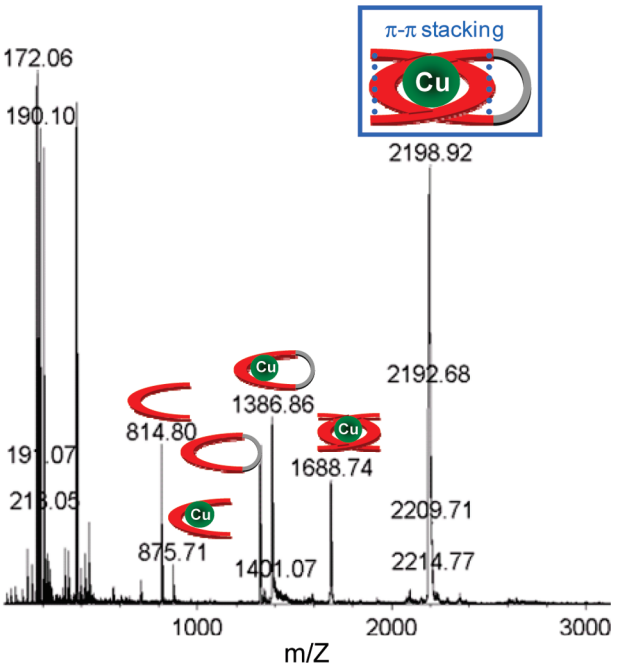

Figure 6. MALDI-TOF-MS spectrum of a solution containing *o*AB-O13, oAB-2OH, and $[Cu(CH_3CN)_4]BF_4$.

Analysis of the absorption spectral changes of *o*AB-O13 (1.0×10^{-5} M) in CH_2Cl_2 upon thermal cis-to-trans isomerization at 298 K in the dark also indicated that k_1 was larger than k_2 (see Supporting Information, Figures S2 and S3).

Coordination Behavior of *o*AB-O13 to Copper. The coordination of *o*AB-O13 to Cu(I) was examined using ^{1}H NMR and UV−vis spectroscopy. When *trans*$_2$-*o*AB-O13 and $[Cu(CH_3CN)_4]BF_4$ were mixed in CD_2Cl_2, the ^{1}H NMR peaks broadened (Figure 5a), indicating that the copper was coordinated by not only the bipyridine unit but also loosely by the polyether chain. When a noncyclic ligand, *trans*$_2$-*o*AB-2OH, was added to the mixture, the signals became sharp and the ^{t}Bu peak shifted upfield (Figure 5b). The ^{t}Bu upfield shift was attributed to shielding caused by interligand $\pi-\pi$ stacking, which stabilized the structure of $[Cu(trans_2\text{-}oAB\text{-}O13)(trans_2\text{-}oAB\text{-}2OH)]BF_4$ and bound stably to the copper ion, sharpening the ^{1}H NMR peaks. The formation of $[Cu(oAB\text{-}O13)(oAB\text{-}2OH)]BF_4$ was confirmed by the MALDI-TOF-MS spectrum of this sample (Figure 6). These results indicated that the *o*AB-O13 ring was so

dx.doi.org/10.1021/ic200145h |*Inorg. Chem.* 2011, 50, 4925–4933

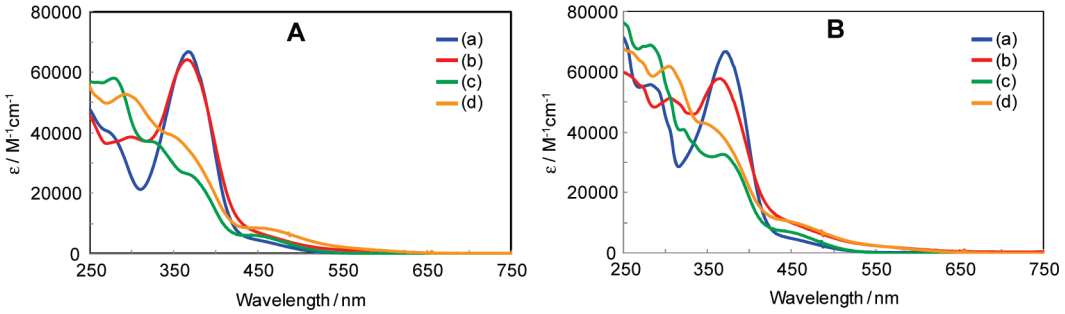

Figure 7. (A) UV−vis spectra of (a) *o*AB-O13 (1.3×10^{-5} M) in CH_2Cl_2, (b) after addition of 1 equiv of $[Cu(CH_3CN)_4]BF_4$, (c) *o*AB-O13 (8.7×10^{-6} M) after irradiation at 365 nm for 5 min, and (d) after addition of $[Cu(CH_3CN)_4]BF_4$. (B) UV−vis spectra of (a) *o*AB-bpy (1.3×10^{-5} M) in CH_2Cl_2, (b) after addition of 1 equiv of $[Cu(CH_3CN)_4]BF_4$, (c) *o*AB-bpy (1.4×10^{-5} M) after irradiation at 365 nm for 5 min, and (d) after addition of $[Cu(CH_3CN)_4]BF_4$.

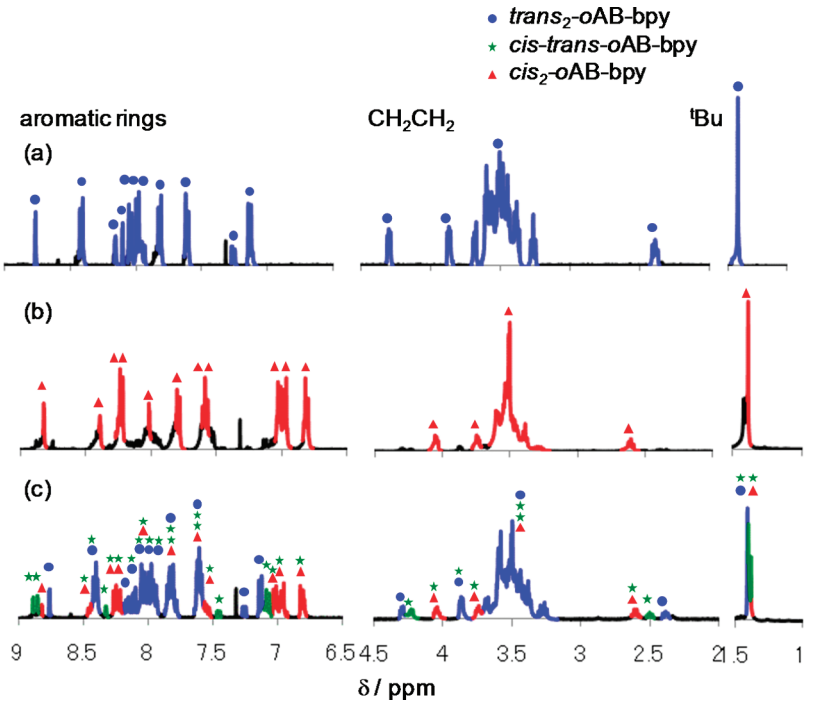

Figure 8. ^{1}H NMR spectral changes of *o*AB-bpy (5.5×10^{-3} M) in CD_2Cl_2 (a) initially, (b) after irradiation at 365 nm for 1 h, and (c) after further irradiation at 436 nm for 1 h.

large and soft that *o*AB-2OH could insert it and, thus, could coordinate to Cu(I).

The UV−vis absorption spectrum of *o*AB-O13 in CH_2Cl_2 showed an intense band at 365 nm (Figure 7a), ascribed to the $\pi-\pi^*$ transition of the azobenzene moiety. The $n-\pi^*$ transition band was observed in the visible region from 400 to 550 nm. After addition of 1 equiv of $[Cu(CH_3CN)_4]BF_4$, the $\pi-\pi^*$ transition band decreases a little (Figure 7b). This decrease showed the interaction between *o*AB-O13 and Cu(I) ion. The absorbance in the visible region from 400 to 550 nm increased. This increase was attributed to the d-π^* transition (MLCT) band,[7] generated through the formation of the complex. The absorption spectrum of the cis complex was gained by two steps; first, oAB-O13 was transferred to the cis form under 365-nm light irradiation, then, $[Cu(CH_3CN)_4]BF_4$ was added. The $\pi-\pi^*$ transition band decreased and the $n-\pi^*$ transition band increased under the UV irradiation (Figure 7c), indicating the trans-to-cis isomerization of azobenzene moieties. During the addition of Cu(I) ion, the $\pi-\pi^*$ transition band increased because the cis-to-trans isomerization took place a little, and the absorbance in the visible region from 400 to 550 nm, attributed to the d-π^* transition (MLCT) band, increased through the formation of the complex (Figure 7d).

Isomerization of *o*AB-bpy. The photoisomerization behavior of *trans*$_2$-*o*AB-bpy in CD_2Cl_2 was monitored by NMR (Figure 8). New signals were observed after 365 nm light irradiation, indicating that trans-to-cis isomerization had taken place. Evidence for both the *cis*$_2$ form and the *cis-trans* form was observed, suggesting that isomerization proceeded stepwise via the *cis-trans* form. The ratios of the *trans*$_2$ form, the *cis-trans* form, and the *cis*$_2$ form were 0.18:0.12:0.70. Isomerization in the reverse direction was observed upon 436 nm light irradiation. Irradiation with 365 or 436 nm light for 1 h produced a photostationary state solution in which the ratios of the *trans*$_2$ form, the *cis-trans* form,

dx.doi.org/10.1021/ic200145h |*Inorg. Chem.* 2011, 50, 4925–4933

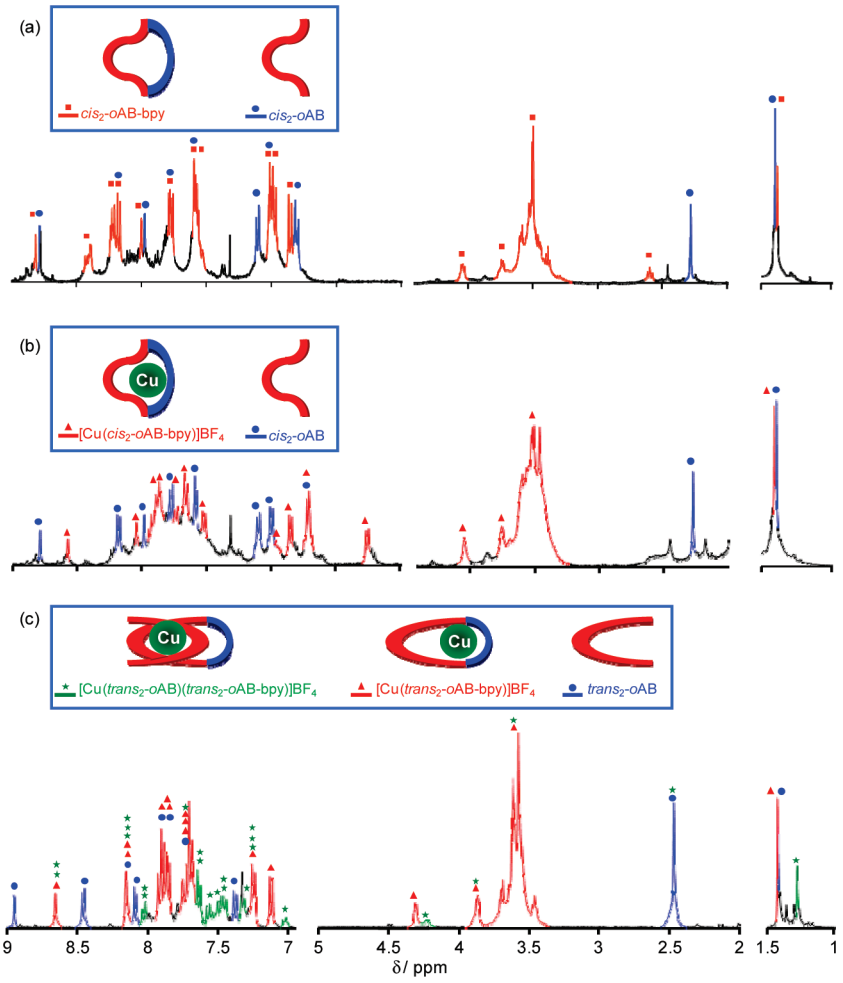

Figure 9. ^{1}H NMR spectral changes of *o*AB-bpy (4.6×10^{-3} M), *o*AB (4.6×10^{-3} M), and $[Cu(CH_3CN)_4]BF_4$ (4.6×10^{-3} M) in CD_2Cl_2 (a) before addition of $[Cu(CH_3CN)_4]BF_4$, (b) after addition of $[Cu(CH_3CN)_4]BF_4$ in the cis form, and (c) after addition of $[Cu(CH_3CN)_4]BF_4$ in the trans form.

and the *cis*$_2$ form were 0.36:0.43:0.21. The azobenzene moieties thermally isomerized from the cis to the trans forms, and the original state (or *o*AB-O13) was recovered upon heating the solution at 40 °C in the dark for 12 h.

The ^{1}H NMR spectra of *trans*$_2$-*o*AB-bpy and *cis*$_2$-*o*AB-bpy in CD_2Cl_2 were compared in Supporting Information, Table S4. The H*d* peak shifted downfield and the H*g* and H*h* peaks shifted upfield through the trans-to-cis isomerization. These shifts were the same as those of *o*AB-O13, indicating the same conformational changes of the bipyridine moiety attached to the azobenzene units.

Synchronization of Isomerization and Ligand Exchange in [Cu(*o*AB-bpy)]$^+$. The UV−vis spectral change of *o*AB-bpy through trans-to-cis isomerization by 365 nm light irradiation, followed by coordination to Cu(I) by adding 1 equiv of $[Cu(CH_3CN)_4]BF_4$ was similar with that of *o*AB-O13 (compare Figure 7 A and B). The isomerization and ligand exchange reactions in the *o*AB-bpy complex of copper were synchronized as follows. First, *trans*$_2$-*o*AB-bpy and *trans*$_2$-*o*AB in CD_2Cl_2 were converted to the *cis*$_2$ and *cis-trans* forms under 365 nm light irradiation for 1 h. The cis form of azobenzene was present at 83% in *o*AB-bpy and 76% in *o*AB, based on the ^{1}H NMR results (Figure 9a). When $[Cu(CH_3CN)_4]BF_4$ was added to this solution, the ^{1}H NMR signals of *o*AB were unchanged. However, the peaks corresponding to *o*AB-bpy disappeared and new peaks appeared (Figure 9b). The new peaks in the aromatic ring region were upfield relative to the peaks from *o*AB-bpy, indicating coordination of *o*AB-bpy to the copper ion. ESI-MS data also indicated formation of $[Cu(oAB\text{-}bpy)]BF_4$ (Supporting Information, Figure S4a). Next, $[Cu(oAB\text{-}bpy)]BF_4$ and *o*AB were converted to the *trans*$_2$ form by heating the solution at 40 °C in the dark for 15 h. ^{1}H NMR peaks for the free *trans*$_2$-*o*AB were observed, although signals of the free *trans*$_2$-*o*AB-bpy were not observed (Figure 9c). Instead, the peaks attributed to $[Cu(trans_2\text{-}oAB\text{-}bpy)]BF_4$ appeared (red line in Figure 9c). The green spectrum in Figure 9c showed that the ^{t}Bu peak was shifted upfield, indicating the presence of interligand $\pi-\pi$ stacking. These peaks were different from those of $[Cu(trans_2\text{-}oAB)_2]BF_4$ and thus were attributable to $[Cu(trans_2\text{-}oAB)(trans_2\text{-}oAB\text{-}bpy)]BF_4$. This attribution was supported by the observation of peaks due to $[Cu(oAB)(oAB\text{-}bpy)]^+$ in the ESI-MS spectrum (Supporting Information, Figure S4b). The ratios of $[Cu(trans_2\text{-}oAB)(trans_2\text{-}oAB\text{-}bpy)]BF_4$:$[Cu(trans_2\text{-}oAB\text{-}bpy)]BF_4$:*trans*$_2$-*o*AB, calculated from the ^{1}H NMR spectrum, were 0.21:1.0:1.0. According to the formation of $[Cu(trans_2\text{-}oAB)(trans_2\text{-}oAB\text{-}bpy)]BF_4$, the ratio of *trans*$_2$-*o*AB became

dx.doi.org/10.1021/ic200145h |*Inorg. Chem.* 2011, 50, 4925–4933

smaller. The fact that the ratio of [Cu(*trans*$_2$-*o*AB-bpy)]BF_4: *trans*$_2$-*o*AB was 1:1 also indicated the formation of [Cu(*trans*$_2$-*o*AB)(*trans*$_2$-*o*AB-bpy)]BF_4. This implied that the conversion from the cis form to the trans form of the azobenzene moieties caused the penetration of *o*AB into *o*AB-bpy. In other words, the isomerization and ligand exchange reactions were synchronized.

CONCLUSIONS

Novel cyclic ligands with azobenzene moieties and bipyridine moieties, *o*AB-O13 and *o*AB-bpy, were synthesized, and their photochemical and coordination properties were investigated. Both *o*AB-O13 and *o*AB-bpy underwent reversible photoisomerization. ^{1}H NMR and MS measurements showed that mixing of [Cu(*trans*$_2$-*o*AB-O13)]BF_4 with *o*AB-2OH yielded [Cu(*trans*$_2$-*o*AB-2OH)-(*trans*$_2$-*o*AB-O13)]BF_4. This product indicated that the ring size of *trans*$_2$-*o*AB-O13 was sufficiently large and soft that *o*AB-2OH could penetrate it and coordinate to the copper ion. When [Cu(CH_3CN)$_4$]BF_4 was added to a solution of *cis*$_2$-*o*AB-bpy and *cis*$_2$-*o*AB in CD_2Cl_2, [Cu(*cis*$_2$-*o*AB-bpy)]BF_4 and *cis*$_2$-*o*AB formed. Upon conversion of these compounds to their *trans*$_2$ forms, *o*AB penetrated into *o*AB-bpy. This result implied that the isomerization and ligand exchange reactions were synchronized.

EXPERIMENTAL SECTION

*o*AB-2OH,[6] pentaethylene glycol ditosylate,[8] dodecaethylene glycol ditosylate (O13-Ts),[8] 4,4′-(2,2′-bipyridine-5,5′-diyl)dibutan-1-ol,[9] and tetrakis(acetonitrile)copper(I) tetrafluoroborate[10] were prepared according to procedures reported in the literature. All reagents were purchased from Tokyo Kasei, except for acetic acid (from Kanto Chemicals) and cesium carbonate (from Wako Chemicals), and were used as received.

NMR spectra were recorded using JEOL AL-400 or ECX-400 spectrometers. MALDI-TOF MS spectra were recorded using a KRATOS AXIMA-CFR. ESI-TOF MS spectra were recorded using a Micromass-LCT spectrometer. UV−vis spectra were recorded using a Hewlett-Packard 8453 spectrometer. Photoirradiation experiments were performed using a super high-pressure mercury lamp (USHIO-500D) as a light source, and each emission line was separated with a monochromator (Jasco CT-10T, $\Delta\lambda = \pm 30$ nm).

***o*AB-O13.** A solution of *o*AB-2OH (190 mg, 0.234 mmol) and O13-Ts (200 mg, 0.234 mmol) in dry DMF (80 mL) was added dropwise over 6 h under N_2 to a suspension of Cs_2CO_3 (200 mg, 0.614 mmol) in dry dimethylformamide (DMF, 40 mL) maintained at 50 °C. After the addition, the solution was stirred and heated for 7 days. The solvent was removed in vacuo. Water (100 mL) was added to the red residue and was extracted with chloroform (3 × 50 mL). The organic layer was collected, dried over Na_2SO_4, and the solvent was removed in vacuo. The residue was subjected to HPLC, and *o*AB-O13 was obtained as an orange powder (21 mg, 6.9%).

^{1}H NMR (400 MHz, $CDCl_3$, TMS): δ 8.47 (d, 4H, J = 8.8 Hz, Ph), 8.21 (s, 2H, py), 8.12 (s, 2H, py), 8.07 (d, 4H, J = 8.8 Hz, Ph), 7.96 (d, 4H, J = 9.2 Hz, Ph), 7.78 (d, 4H, J = 8.4 Hz, Ph), 7.60 (d, 4H, J = 8.4 Hz, Ph), 7.09 (d, 4H, J = 9.2 Hz, Ph), 4.29 (t, 4H, J = 4.8 Hz, CH_2), 3.90 (t, 4H, J = 4.8 Hz, CH_2), 3.80−3.43 (m, 44H, OCH_2CH_2O), 1.42 (s, 18H, ^{t}Bu).

^{13}C NMR (100 MHz, $CDCl_3$, TMS): δ 161.40 (Ph), 157.44 (py), 157.08 (py), 153.03 (Ph), 152.51 (Ph), 150.24 (py), 147.18 (Ph), 141.07 (Ph), 135.67 (Ph), 127.99 (Ph), 126.91 (Ph), 126.14 (Ph), 124.75 (Ph), 123.00 (Ph), 119.15 (py), 118.26 (py), 115.12 (Ph), 70.94−67.81 (OCH_2CH_2O), 34.79 (^{t}Bu), 31.31 (^{t}Bu).

MALDI-TOF-MS (m/z): $[M+H]^+$ calcd for $C_{78}H_{95}N_6O_{13}$, 1323.67; found, 1323.67.

Anal. Calcd for $C_{78}H_{94}N_6O_{13}\cdot 2H_2O$: C, 68.90; H, 7.26; N, 6.18. Found: C, 68.99; H, 7.22; N, 5.75.

bpy-Ts. A mixture of 4,4′-(2,2′-bipyridine-5,5′-diyl)dibutan-1-ol (1.33 g, 4.43 mmol) and NaH (1.00 g, 41.7 mmol) in dry tetrahydrofuran (THF, 35 mL) was stirred for 1 h under N_2. To the pale brown solution was added pentaethylene glycol ditosylate (7.06 g, 12.9 mmol) in dry THF (35 mL). After refluxing for 18 h, water was added to destroy residual NaH, and the solvent was removed in vacuo. The dark brown residue was dissolved in water (100 mL) and extracted with chloroform (5 × 50 mL). The organic layer was collected, dried over Na_2SO_4, and the solvent was removed in vacuo. The residue was subjected to column chromatography (silica gel, $CHCl_3$:MeOH = 19:1) and bpy-Ts was obtained as a pale brown liquid (1.12 g, 24.1%).

^{1}H NMR(400 MHz, $CDCl_3$, TMS): δ 8.48 (s, 2H, py), 8.25 (d, 2H, J = 8.0 Hz, py), 7.80 (d, 4H, J = 8.2 Hz, Ph), 7.62 (d, 2H, J = 8.0 Hz, py), 7.34 (d, 4H, J = 8.2 Hz, Ph), 4.15 (t, 4H, J = 4.6 Hz, $TsOCH_2$), 3.69−3.57 (m, 36H, OCH_2CH_2O), 3.49 (t, 4H, J = 6.4 Hz, OCH_2), 2.68 (t, 4H, J = 7.6 Hz, $pyCH_2$), 2.44 (s, 6H, CH_3), 1.75−1.65 (m, 8H, CH_2CH_2).

MALDI-TOF-MS (m/z): $[M+H]^+$ calcd for $C_{52}H_{77}N_2O_{16}S_2$, 1049.47; found, 1049.40.

***o*AB-bpy.** A mixture of *o*AB-2OH (106 mg, 0.130 mmol) and bpy-Ts (145 mg, 0.138 mmol) in dry DMF (50 mL) was added dropwise over 5 h under N_2 to a suspension of Cs_2CO_3 (211 mg, 0.648 mmol) in dry DMF (50 mL) maintained at 50 °C. After the addition, the solution was stirred and heated for 8 days. The solvent was removed in vacuo. Water (100 mL) was added to the red residue, and the solution was extracted with chloroform (3 × 40 mL). The organic layer was collected, dried over Na_2SO_4, and the solvent was removed in vacuo. The residue was subjected to HPLC, and *o*AB-bpy was obtained as an orange powder (14 mg, 7.1%).

^{1}H NMR (400 MHz, CD_2Cl_2): δ 8.76 (s, 2H, py), 8.41 (d, 4H, J = 8.7 Hz, Ph), 8.15 (s, 2H, py), 8.10 (s, 2H, py), 8.04 (d, 4H, J = 8.7 Hz, Ph), 7.99 (d, 4H, J = 8.7 Hz, Ph), 7.94 (d, 2H, J = 7.9 Hz, py), 7.82 (d, 4H, J = 8.7 Hz, Ph), 7.61 (d, 4H, J = 8.7 Hz, Ph), 7.26 (d, 2H, J = 7.9 Hz, py), 7.13 (d, 4H, J = 8.7 Hz, Ph), 4.30 (t, 4H, J = 4.4 Hz, CH_2), 3.87 (t, 4H, J = 4.4 Hz, CH_2), 3.70−3.36 (m, 32H, OCH_2CH_2O), 3.26 (t, 4H, J = 6.6 Hz, CH_2), 2.39 (t, 4H, J = 7.6 Hz, CH_2), 1.46 (m, 8H, CH_2CH_2), 1.42 (s, 18H, ^{t}Bu).

^{13}C NMR (100 MHz, $CDCl_3$, TMS): δ 161.38 (Ph), 156.51 (py), 156.06 (py), 155.42 (py), 153.00 (Ph), 152.36 (Ph), 150.19 (py), 148.61 (py), 147.20 (Ph), 141.23 (Ph), 136.47 (Ph), 133.75 (py), 129.81 (py), 127.80 (Ph), 127.04 (Ph), 126.13 (Ph), 124.84 (Ph), 123.04 (Ph), 120.77 (py), 118.80 (py), 118.24 (py), 114.86 (Ph), 71.32−67.72 (OCH_2CH_2O), 34.79 (^{t}Bu), 31.35 (^{t}Bu).

MALDI-TOF-MS (m/z): $[M+H]^+$ calcd for $C_{92}H_{109}N_8O_{12}$, 1517.82; found, 1517.48.

Anal. Calcd for $C_{92}H_{114}N_8O_{15}\cdot 3H_2O$: C, 70.29; H, 7.31; N, 7.13. Found: C, 70.28; H, 7.15; N, 6.82.

ASSOCIATED CONTENT

Supporting Information. Further details are given in Tables S1−S4 and Figures S1−S4. This material is available free of charge via the Internet at http://pubs.acs.org.

AUTHOR INFORMATION

Corresponding Author

*Phone: 81-3-5841-4346. Fax: 81-3-5841-4489. E-mail: nisihara@chem.s.u-tokyo.ac.jp.

ACKNOWLEDGMENT

This work was supported by Grants-in-Aid for Scientific Research from MEXT, Japan (Nos. 20245013 and 21108002,

area 2107), and the Global COE Program for Chemistry Innovation.

REFERENCES

(1) Molecular machines special issue: *Acc. Chem. Res.* **2001**, *34*, 409.

(2) (a) Fraysse, S.; Coudret, C.; Launay, J.-P. *Eur. J. Inorg. Chem.* **2000**, 1581–1590. (b) Sakamoto, R.; Murata, M.; Nishihara, H. *Angew. Chem., Int. Ed.* **2006**, *45*, 4793–4795. (c) Cardenas, D. J.; Livoreil, A.; Sauvage, J.-P. *J. Am. Chem. Soc.* **1996**, *118*, 11980–11981. (d) Bissell, R. A.; Córdova, E.; Kaifer, A. E.; Stoddart, J. F. *Nature* **1994**, *369*, 133–137. (e) Durola, F.; Lux, J.; Sauvage, J.-P.; Wenger, O. S. *Supramol. Chem.* **2011**, *23*, 42–52.

(3) (a) Muraoka, T.; Kinbara, K.; Aida, T. *Nature* **2006**, *440*, 512–515. (b) Kai, H.; Nara, S.; Kinbara, K.; Aida, T. *J. Am. Chem. Soc.* **2008**, *130*, 6725–6727.

(4) (a) Kurihara, M.; Hirooka, A.; Kume, S.; Sugimoto, M.; Nishihara, H. *J. Am. Chem. Soc.* **2002**, *124*, 8800–8801. (b) Nihei, M.; Kurihara, M.; Mizutani, J.; Nishihara, H. *J. Am. Chem. Soc.* **2003**, *125*, 2964–2973. (c) Nagashima, S.; Murata, M.; Nishihara, H. *Angew. Chem., Int. Ed.* **2006**, *45*, 4298–4301. (d) Sakamoto, R.; Murata, M.; Nishihara, H. *Angew. Chem., Int. Ed.* **2006**, *45*, 4793–4795. (e) Muratsugu, S.; Kume, S.; Nishihara, H. *J. Am. Chem. Soc.* **2008**, *130*, 7204–7205. (f) Kume, S.; Nishihara, H. *Dalton Trans.* **2008**, 3260–3271. (g) Kume, S.; Nishihara, H. *Struct. Bonding (Berlin)* **2007**, *123*, 79–112.

(5) Kume, S.; Murata, M.; Ozeki, T.; Nishihara, H. *J. Am. Chem. Soc.* **2005**, *127*, 490–491.

(6) Umeki, S.; Kume, S.; Nishihara, H. *Chem. Lett.* **2010**, *39*, 204–205.

(7) (a) McMillin, D. R.; Kirchhoff, J. R.; Goodwin, K. V. *Coord. Chem. Rev.* **1985**, *64*, 83–92. (b) Everly, R. M.; McMillin, D. R. *J. Phys. Chem.* **1991**, *95*, 9071–9075. (c) Meyer, M.; Albrecht-Gary, A.-M.; Dietrich-Buchecker, C. O.; Sauvage., J.-P. *Inorg. Chem.* **1999**, *38*, 2279–2287.

(8) (a) Ouchi, M.; Inoue, Y.; Liu, Y.; Nagamune, S.; Nakamura, S.; Wada, K.; Hakushi, T. *Bull. Chem. Soc. Jpn.* **1990**, *63*, 1260–1262. (b) Ouchi, M.; Inoue, Y.; Kanazaki, T.; Hakushi, T. *J. Org. Chem.* **1984**, *49*, 1408–1412.

(9) (a) Lindner, E.; Veigel, R.; Ortner, K.; Nachtigal, C.; Steimann, M. *Eur. J. Inorg. Chem.* **2000**, 959–969. (b) Hodgson, G. L.; MacSweeney, D. F.; Money, T. *J. Chem. Soc., Perkin Trans.* **1973**, 2113–2130.

(10) Merril, C. L.; Wilson, L. J.; Thamann, T. J.; Loehr, T. M.; Ferris, N. S.; Woodruff, W. H. *J. Chem. Soc., Dalton. Trans.* **1984**, 2207–2221.